Available online at www.sciencedirect.com

SciVerse ScienceDirect

Ceramics International 39 (2013) 1469–1476

CERAMICS INTERNATIONAL

www.elsevier.com/locate/ceramint

Encapsulation of CoS nanoparticles in PAN electrospun nanofibers: Effective and reusable catalyst for ammonia borane hydrolysis and dyes photodegradation

Gopal Panthi[a], Nasser A.M. Barakat[a,c,*], Khalil Abdelrazek Khalil[d], Ayman Yousef[a], Kyung-Soo Jeon[b], Hak Yong Kim[b]

[a]*Department of Bionano System Engineering, College of Engineering, Chonbuk National University, Jeonju 561-756, Republic of Korea*
[b]*Organic Materials and Fiber Engineering Department, Chonbuk National University, Jeonju 561-756, Republic of Korea*
[c]*Chemical Engineering Department, Minia University, El-Minia, Egypt*
[d]*Mechanical Engineering Department, (NPST), King Saud University, P.O. Box 800, Riyadh 11421, Saudi Arabia*

Received 9 July 2012; received in revised form 27 July 2012; accepted 27 July 2012
Available online 16 August 2012

Abstract

In this study, the effective cobalt sulfide NPs were successfully encapsulated inside polyacrylonitrile (PAN) electrospun nanofibers. Typically, the solid NPs were in-situ synthesized by addition of ammonium sulfide drops to PAN/cobalt acetate solution. Electrospinning of the obtained colloid led to obtain good morphology polymeric nanofibers containing CoS NPs. Complete sheathing of the active nanoparticles did not affect their catalytic activity as the prepared mats revealed high performance toward hydrogen release from ammonia borane hydrolysis. Moreover, as a photocatalyst, a mat containing 2 wt% CoS could catalyze oxidation of methylene blue dye to be completely eliminated within 15 min. Furthermore, the introduced nanofibers photocatalytically enhanced complete degradation of the methyl red dye within relatively short time. The experimental results indicated that the optimum CoS content is 2 wt%, more increase in the concentration of the solid NPs leads to particles aggregation and consequently decrease the surface area. Beside the good activity obtained, the introduced immobilization strategy is considered an acceptable methodology to overcome the secondary pollution of the nanostructural photocatalysts because of the easy separation feasibility.

Keywords: Photocatalysts immobilization; Electrospinning; Cobalt sulfide; Ammonia borane

1. Introduction

The study on inorganic–organic nanocomposites has become an extremely active area during the past decade because of their unusual optical, electrical, magnetic and mechanical properties with a wide variety of applications in materials science, such as superconductors, magnetic materials, catalysts, and luminescent materials [1–5]. As the representatives of these materials, polymer/metal sulfide nanocomposites are of continuous interest because they can exhibit various intriguing properties being far superior to those of the individual components [6], which results in functional materials having potential applications in diverse areas. In such nanostructured composites, the polymer matrix provides the processability and flexibility, and the inorganic nanoparticles can not only enhance the mechanical properties of the host polymer but also provide extraordinary properties compared to their bulk counterparts [7,8].

Among the various metallic compounds, metal sulfides have distinct catalytic activity. Cobalt sulfides form a group of II–IV semiconductor materials with considerable potential for applications in electronic devices. They can be used in solar devices [9], ultra-high-density magnetic recording

*Corresponding author at: Chonbuk National University, Organic Materials and Fiber Engineering Department, Jeonju 561-756 Korea. Tel.: +82 63 270 2363; fax: +82 63 270 2348.
E-mail addresses: nasser@jbnu.ac.kr (N.A.M. Barakat), khy@jbnu.ac.kr (H.Y. Kim).

0272-8842/$ - see front matter © 2012 Elsevier Ltd and Techna Group S.r.l. All rights reserved.
http://dx.doi.org/10.1016/j.ceramint.2012.07.091

material [10], anodes for Li-ion batteries [11] and catalysts for hydrodesulphurization and dehydrodearomatization [12]. Due to its proper band gap and good adsorption properties, CoS can be used as photocatalyst. Photocatalytic treatment of organic compounds in wastewater using semiconductors has proven to be a promising green technology for environmental purification as they provide an interface with an aqueous medium and induce an advanced oxidation process. In the literature, many reports about nanostructural photocatalytic materials have been introduced. Although, some of nanomaterials revealed good performance, the researchers ignore the secondary pollution of the introduced photocatalyst as the separation of the nanoparticles after achieving the treatment process is not an easy task. Therefore, immobilization of the photocatalyst on a proper substrate might be an effective strategy to overcome the separation dilemma. The surface area is the main capital of the nanostructures; accordingly the chosen substrate should not affect the surface area advantage.

Electrospinning has attracted much attention as a simple and versatile technique capable of generating continuous nanofibers with novel properties including high surface-to-volume ratio, good mechanical properties and high aspect ratio [13,14]. Consequently, electrospun nanofibers found intriguing applications in tissue engineering scaffolds [15], wound dressing [16], sensors[17], catalyst [18,19], and environmental remediation [20]. According to the aforementioned features, electrospun nanofibers can be a proper substrate for the photocatalytic nanostructures.

In this study, the active cobalt sulfide (CoS) nanoparticles have been incorporated inside polyacrylonitrile (PAN) electrospun nanofibers. Synthesizing of the solid NPs has been achieved by addition of ammonium sulfide solution to PAN/cobalt acetate sol–gel. Interestingly, the proposed incorporation strategy did not affect the photocatalytic activity of CoS NPs. Moreover, the hybrid mats could be utilized as effective catalyst to hydrolyze ammonia borane.

2. Experimental procedure

2.1. Materials

Cobalt acetate tetrahydrate (CoAc, reagent grade, extra pure, Junsei Chemicals Co. Ltd., Japan), N,N-dimethylformamide (DMF, 99.5 assay, Showa Chemical Ltd., Japan), polyacrylonitrile (PAN, MW 150,000 g/mol, Sigma–Aldrich), ammonium sulfide (40–48 wt% solution in water, Sigma–Aldrich), methylene blue (MB) and methyl red (MR) (Showa Chemical Ltd., Japan) were used in this study without further treatment. Ammonia borane complex (AB, assay 97.0%) was purchased from Aldrich.

2.2. Preparation of CoS-doped PAN hybrid electrospun nanofiber mat

Cobalt sulfide (CoS)/polyacrylonitrile (PAN) colloidal solution was prepared by the following procedure. First, 10 wt% PAN solution was prepared by dissolving the polymer granules in N,N-dimethylformamide (DMF) with vigorous stirring for 12 h at room temperature to form homogenous solution. The metallic precursor was dissolved in the minimum amount of DMF then mixed with the PAN solution. Solutions having 1, 2, and 3 wt% of cobalt acetate (CoAc) (based on polymer solution) were prepared. The solutions were kept under stirring for 2 h to ensure good mixing. Then 0.25 ml of ammonium sulfide was carefully added in a drop wise manner to every solution with vigorous stirring to synthesize the fine dispersion of CoS nanoparticles. Electrospinning of all formulations was carried out at 15 kV and 15 cm distance between the collector and the tip of the syringe. Conventional electrospinning setup was used in the study; the solution was filled in a syringe which was inclined horizontally in a way preventing pouring the solution. Finally, the formed nanofiber mats were dried for 24 h at 60 °C under vacuum oven. Hereafter, the mats obtained from 1%, 2%, and 3% CoAC were named as m1, m2, and m3, respectively.

2.3. Characterization

The surface morphology of the hybrid nanofibers was studied by a JEOL JSM-5900 scanning electron microscope. TEM images of the nanofibers containing CoS nanoparticles (NPs) were obtained via transmission electron microscopy (TEM, JEM-2010, JEOL, Japan) with a 200 kV accelerating voltage. The samples were prepared by directly collecting the nanofibers on the TEM grid during the electrospinning process. In addition, SEM-EDX and TEM-EDX (JEM-2200, JEOL, Japan) spectra of a CoS-doped PAN hybrid electrospun nanofiber mat were also recorded. Information about the phase and crystallinity was obtained with a Rigaku X-ray diffractometer (XRD, Rigaku, Japan) with Cu Ka (l = 1.540 Å) radiation over Bragg angles ranging from 10° to 80°. Fourier transform infrared (FT-IR) spectra were recorded with KBr pellets using an ABB Bomen MB100 Spectrometer (Bomen, Canada). UV absorbance was measured by UV–vis spectrophotometer (HP 8453 UV–vis spectroscopy system, Germany).

2.4. Photocatalytic activity investigation

The photocatalytic activity of the CoS NPs-doped PAN hybrid electrospun nanofiber mats was evaluated by observing the degradation of methylene blue (MB) and methyl red (MR) dye solutions in a simple photochemical reactor. Prior to irradiation, the suspensions were magnetically stirred for 10 min under dark condition to establish an adsorption/desorption equilibrium between dyes and photo-catalyst surface. In the present investigation, the reactions were carried out in inverted glass bottles under the sunlight. The experiment was conducted in a natural atmospheric environment on a sunny day (between 11 AM and 2 PM) in May (the average amount of solar radiation 16.21 MJ/m^2). For the photodegradation experiments, 50 ml of the dye solution (10 ppm concentration) was

treated by 100 mg of CoS NPs-doped PAN hybrid electrospun nanofiber mats in the glass bottles. In addition, a control experiment with 100 mg of pristine PAN mats and catalyst-free were also carried out to monitor PAN adsorption activity and dye self-degradation, respectively. The samples were taken at regular intervals of time, and the concentration of the dye was measured by recording the absorbance at 663 and 430 nm for MB and MR dye solutions, respectively using a UV–vis spectrophotometer.

2.5. Dehydrogenation of ammonia borane complex

The catalytic activity of introduced nanofibers toward AB hydrolysis was evaluated by measuring the rate of hydrogen generation in a typical water-filled gas buret system. Before starting the catalytic activity test, a jacketed reaction flask (25 mL) containing a Teflon-coated stir bar was placed on a magnetic stirrer and thermostated at a specific temperature. Then, a buret filled with water was connected to the reaction flask to measure the volume of the hydrogen gas to be evolved from the reaction. Next, the 75 mL water containing 100 mg of the synthesized nanofibers was transferred into the reaction flask and 31.5 mg (1 mmol) AB (corresponding to generation of a maximum 3 mmol = 67 mL H_2 gas at 25.0 ± 1 °C and 0.91 atm pressure) was added into the catalyst solution under 600 rpm stirring rate. The volume of hydrogen gas evolved was measured by recording the displacement of water level every minute. The reaction was ceased when the no hydrogen gas generation was observed. For a control experiment, the same experiment was repeated without any catalytic material, it was observed that no appreciable hydrogen gas evolved.

3. Results and discussion

Cobalt sulfide is insoluble in most of the common solvents. Therefore, addition of sulfide ion (S^{-2}) to any solution having cobalt ions leads to form a fine precipitates. From the chemistry point of view, these reactions have high yield as the product is a precipitate; CoS. Accordingly, upon addition of the first drop of ammonium sulfide the solutions directly became turbid. Fig. 1 depicts SEM images of the pristine PAN (Fig. 1a) and m1, m2, and m3 (Fig. 1b–d) nanofiber mats, respectively. As shown in the figures, the fibers diameters of all mats are observed in the range of 500–700 nm. Synthesizing of CoS nanoparticles inside the polymer solution did not affect the nanofibrous morphology as shown in Fig. 1. The complete absence of nanoparticles on the surface of the hybrid nanofibers is confirmed in these SEM images. But the presence of Co and S elements inside m1, m2, and m3 nanofiber mats was confirmed by SEM-EDX as shown in Fig. 1(b^1), (c^1), and (d^1), respectively.

3.1. Phase study

The phase composition and phase structure of the samples were analyzed by power X-ray diffraction. Fig. 2 represents

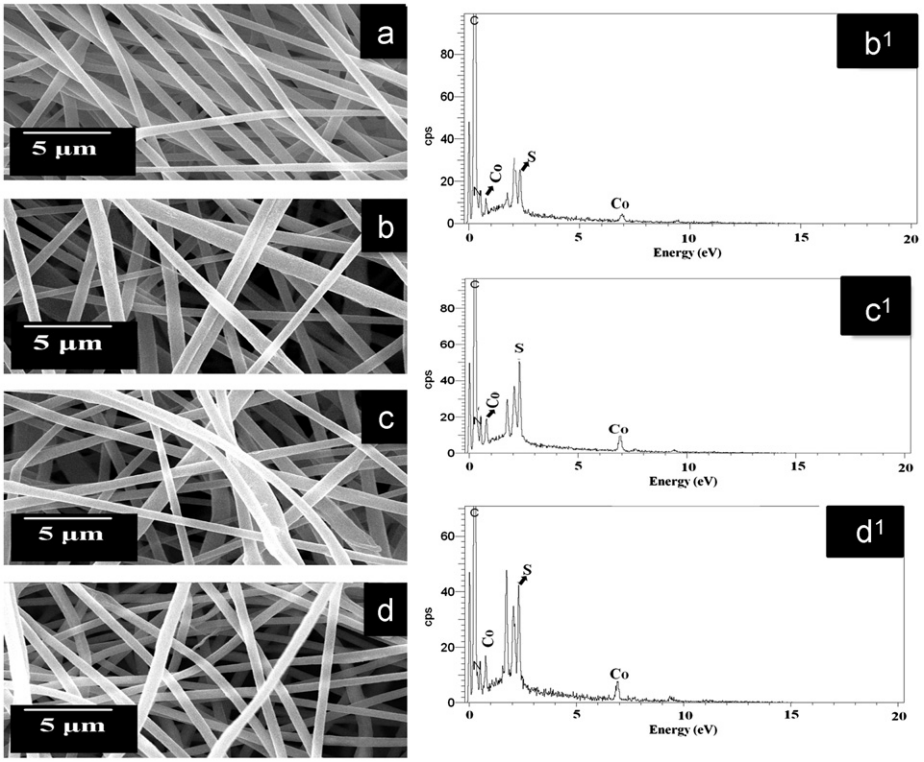

Fig. 1. SEM images of (a) pristine PAN nanofiber mat, (b, c, and d) m1 m2, and m3 nanofiber mats with their EDX Spectrum (b^1, c^1 and d^1), respectively.

the XRD patterns of m3 nanofiber mats. A narrow crystalline peak centers at about 17° and a broad non-crystalline peak (20–30°) can be assigned to the PAN polymer phase [22,23]. But no peaks assigned to CoS can be observed. This may be due to very small size of CoS nanoparticles distributed inside the PAN fibers, however presence of cobalt and sulfur was already confirmed by SEM-EDX (Fig. 2). Moreover, the presence of CoS nanoparticles inside the nanofibers was further confirmed by the TEM image as shown in (Fig. 3). The perfectly crystalline structure of CoS nanoparticles, and the polymer fiber boundary are clearly visible in the HRTEM image shown in (Fig. 3d), the average particle diameter appears to be around 2–5 nm in range. This presence of the nanoparticles inside the polymer can be explained as follows: the position of metallic ions based on electrospun nanofibers should be adjusted by controlling the interaction between the polymer and metallic ions [21]. In our experiment, an electrified polymeric PAN solution with CoS nanoparticles were extruded through a spinneret. During the electrospinning process, the Coulomb repulsion between charged Co^{2+} nanoparticles might be the main factor making the nanoparticles uniformly dispersed and it might increase the interaction with the PAN polymer. Another finding can be obtained from the TEM images that at low CoS content (i.e. 1 wt%, Fig. 3a), few NPs could be observed, the number of observed NPs increases in Fig. 2b (2 wt% CoS). More increase in the CoS content (i.e. 3 wt%) leads to aggregate the formed NPs as shown in Fig. 3c. Fig. 3d represents the HR TEM image of the m2 sample, as shown crystalline dots are shown which can be assigned to CoS. Fig. 4 displays the TEM EDX result of CoS doped PAN nanofibers. As shown, C, Co, and S elements could be detected in the CoS-doped PAN nanofibers (Fig. 4b–d). This further confirmed the presence of CoS nanoparticles inside the nanofibers.

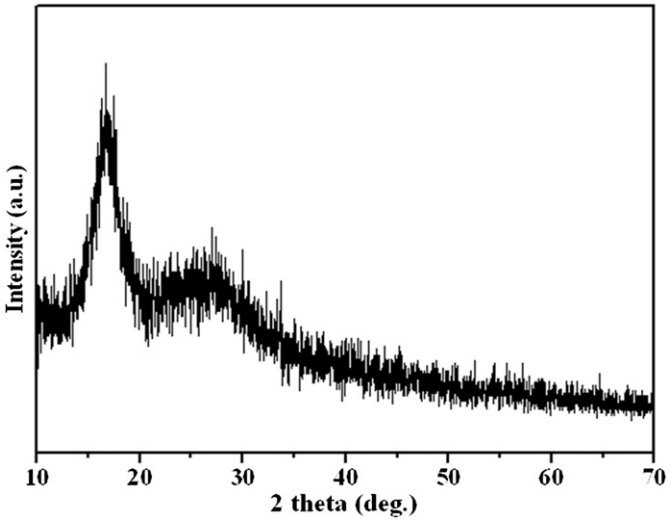

Fig. 2. XRD patterns of m3 nanofiber mat.

FT-IR measurements of pristine PAN and different PAN/CoS nanofibers are demonstrated in Fig. 5. As shown in the spectrum corresponding to pristine PAN nanofibers, the position of all peaks were consistent with the standard infrared spectrum of PAN, the band at about 2242 cm^{-1} was attributed to the stretching vibration of –C≡N group [24]. The characteristic peak at ~2929 $cm^{-1}$was assigned to –CH2– stretching. The peak at ~1450 cm^{-1} was assigned to –CH_2– bending. The spectra PAN/CoS nanofibers were similar with the spectrum of pure PAN. Any shift of the –CN– bond vibration was not detected indicating that there were no conjugate bonds or interaction between –CN– group in the PAN and CoS nanoparticles. So, it could be concluded that the complex between PAN and CoS nanoparticles had been not formed. In other words, the CoS nanoparticles were physically embedded in the PAN nanofibers.

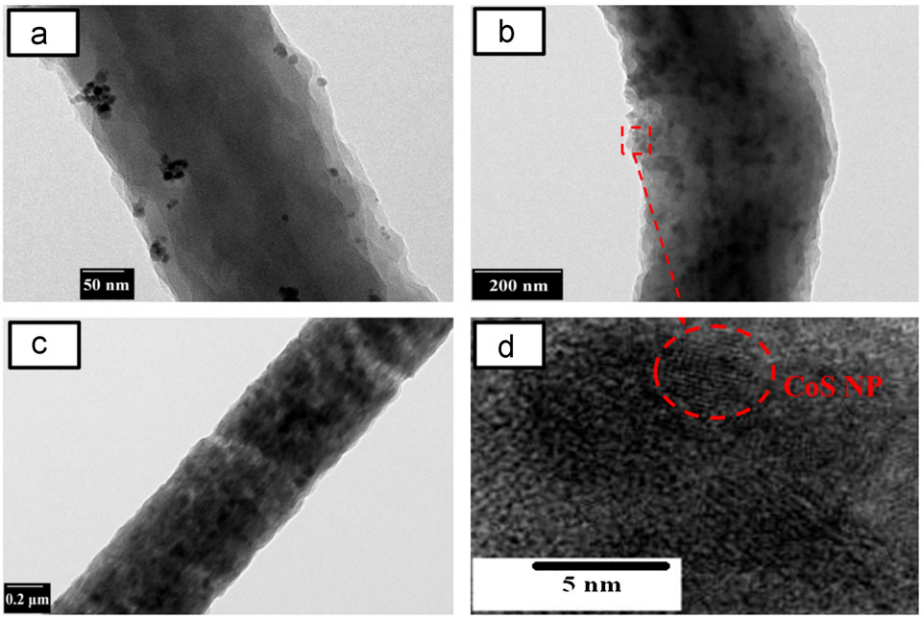

Fig. 3. TEM images of (a) m1, (b) m2, and (c) m3 nanofiber mats. Panel (d) represents the HR TEM image for sample m2.

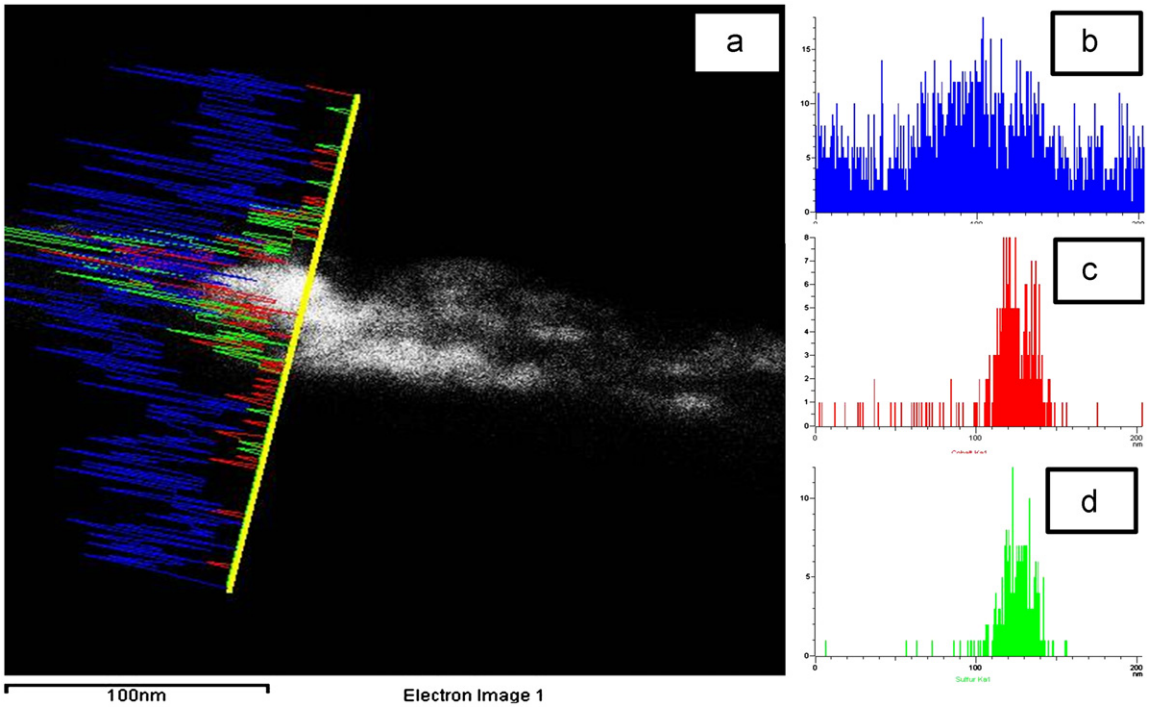

Fig. 4. TEM-EDX of PAN-CoS nanofibers; (a), line-EDX spectra of carbon; (b), cobalt; (c) and sulfur; (d) elements.

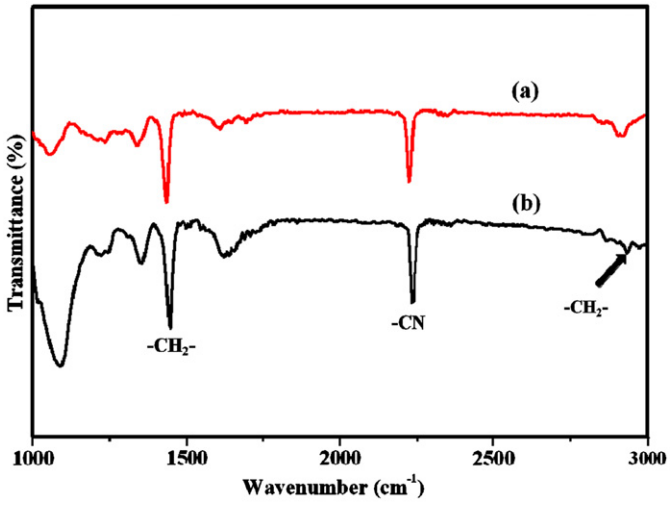

Fig. 5. FTIR spectrum of pristine PAN; (a) and m2; (b) nanofibers.

3.2. Dehydrogenation of ammonia borane complex

Nowadays, there has been growing interest among the researchers toward hydrogen storage which is considered to be the energy harvesting alternative material. Among the reported hydrogen storage materials, ammonia borane (AB) complex drew much attention due to its high hydrogen content (19.6 wt%), thermal stability and potential regenerability [13]. AB releases hydrogen by pyrolysis or a hydrolysis route. The pyrolysis process has been well studied. However, the pyrolysis of solid AB, at potential application temperatures is unable to meet the recent targets and this approach is confounded by the practical disadvantages associated with delivery of a solid material. Recently, the hydrolysis of AB was accomplished by the use of catalytic materials like Ir metal complexes [22], various noble and non-noble metals [23], and ionic liquids [24]. It is noteworthy mentioning that the reported stability of AB was examined in the present study. As shown in Fig. 6a. At 50 °C, with absence of the catalyst, the hydrogen release from AB is negligible. As the metal sulfides in general and CoS in particular have good catalytic activity, the catalytic activities of the synthesized nanofiber mats toward AB hydrolysis have been investigated. As shown in Fig. 6a, the three mats showed good activity toward dehydrogenation of AB in daylight at 50 °C. Reusability of the catalyst is very important character. Fig. 6b indicates that the proposed nanofibers can be reused with the same efficiency as no any change of the catalytic activity was observed upon using the same mat (m2) for another cycle. Another observation can be gained from Fig. 6a that the three mats have little difference in the catalytic activity. The better hydrogen production rate in case of m2 nanofiber mat might be due to high surface area of CoS nanoparticles compared to m1 and m3 nanofiber mats due to the low CoS content and aggregation of the NPs in case of m1 and m3 mats, respectively.

3.3. Photocatalytic activity of PAN/CoS hybrid mats

For photocatalytic activity evaluation under solar light irradiation, the photodegradation of methylene blue (MB) and methyl red (MR) was used as a model reaction. Temporal changes in the concentration of MB and MR were monitored by examining the variations in maximal

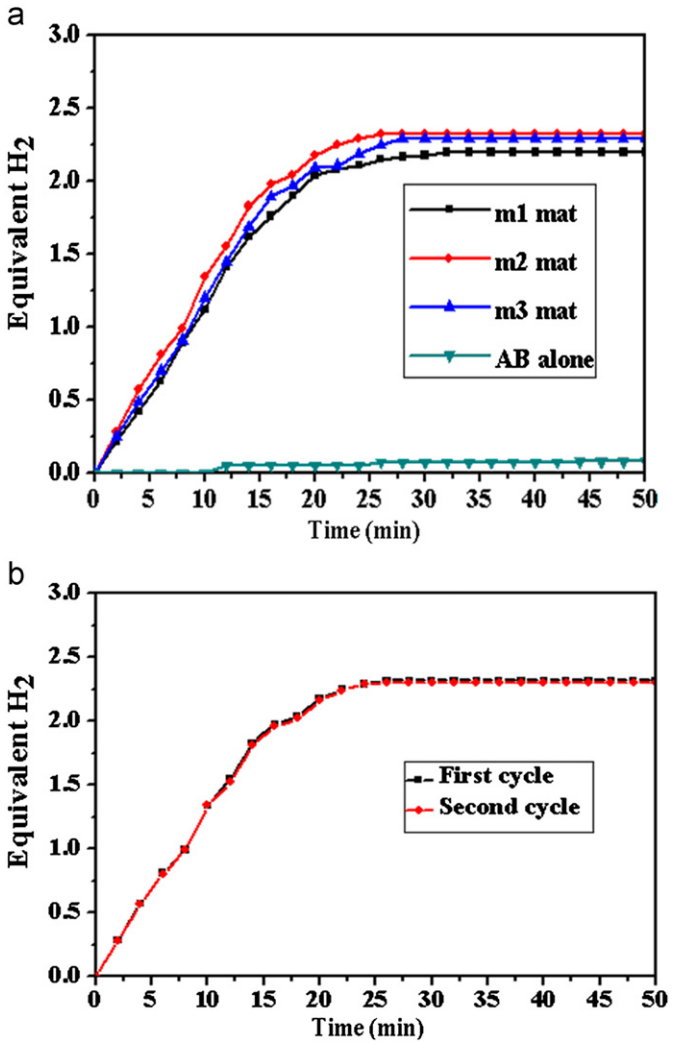

Fig. 6. Hydrogen production studies due to dehydrogenation of ammonia borane by different nanofiber mats; (a) and cycle test of m2 nanofiber mat; (b).

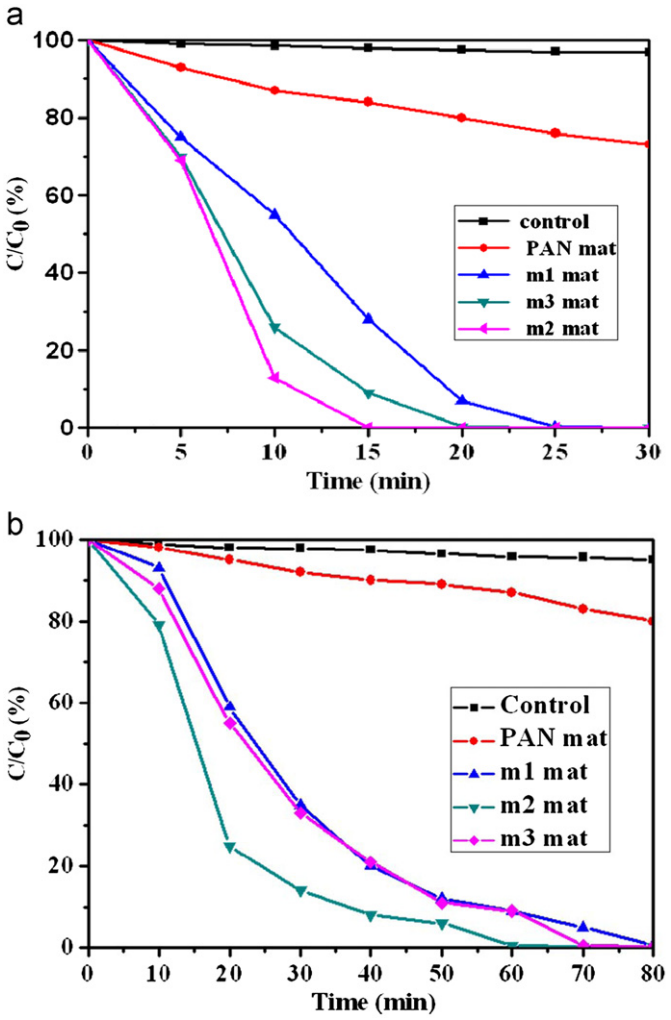

Fig. 7. Decolorization results of (a) methylene blue (MB) and (b) methyl red (MR) dyes using different nanofiber mats.

absorption in UV–vis spectra as shown in the following obtained results. Fig. 7 shows the results of degradation of MB and MR in the presence of the different samples. In order to check the self-degradation of the dyes under the sunlight, the experiment was carried out without presence of the hybrid mats. The absorption property of PAN mat towards both dyes were also evaluated, self degradation and PAN adsorption were found to be very small for both dyes as shown in Fig. 7. From the results, it is clear that the complete degradation of MB by m1, m2, and m3 nanofiber mats occurred within 25, 15, and 20 min, respectively and for MR within 80, 60, and 70 min, respectively. These results, especially with MB which is used as organic pollutant model in the literature, indicate strong photoactivity characteristic of the introduced nanofibers as complete elimination of the dye in 15 min is a distinct finding. Also, MR as azo dye could be not completely oxidized by many reported photocatalyst, in this study the introduced nanofibers successfully eliminated the dye within relatively short time. Again, it was found that m2 nanofiber mat was more effective towards the degradation of both dyes compared to the other two formulations which affirms the aforementioned hypothesis about low active material content and aggregation of the NPs in case of m1 and m3, respectively.

The proposed mechanism of photocatalytic activity of CoS NPs has been introduced in Fig. 8. This figure shows a conceptual illustration of the photodegradation process for the organic pollutants by the hybrid mat. Briefly, the solar radiation leads to excite the electrons from the valence band to the conduction level leaving holes behind. Low recombination between the excited electrons and the formed holes is an important characteristic of the CoS NPs which results in good catalytic activity. Generally sunlight irradiation results in the formation of the electron–hole pairs. Afterward, the holes were ultimately trapped by surface hydroxyl groups (or H_2O) at the catalyst surface to yield $OH^{\bullet}$ radicals. Meanwhile, the dissolved oxygen molecules reacted with the electrons to yield superoxide radical anions, O_2^-, which on protonation generated the hydroperoxy, $HO_2^{\bullet}$, radicals, producing hydroxyl radical $OH^{\bullet}$, which was a strong

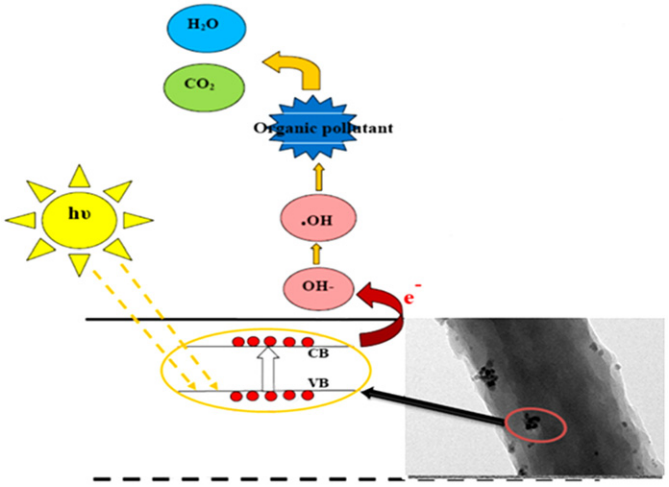

Fig. 8. Schematic illustration shows the photodegradation of organic pollutants using the proposed CoS-doped PAN nanofiber under the solar radiation.

oxidizing agent to decompose the organic dyes. The hydroxyl radical is responsible for the dye degradation. The reactions taking place can be summarized as follows [25].

$$CoS + h\nu \rightarrow e^- + h^+$$

At the conduction band

$$e^- + O_2 \rightarrow O_2^{\bullet -}$$

$$O_2^{\bullet -} + H_2O \rightarrow OH^- + HO_2^{\bullet}$$

$$HO_2^{\bullet} + H_2O \rightarrow H_2O_2 + OH^{\bullet}$$

$$H_2O_2 \rightarrow 2OH^{\bullet}$$

At the valence band

$$h^+ + OH^- \rightarrow OH^{\bullet}$$

Degradation reaction

$$OH^{\bullet} + \text{Organic pollutant} \rightarrow CO_2 + H_2O$$

4. Conclusion

Addition of ammonium sulfide solution to PAN solution containing cobalt acetate leads to in-situ formation of CoS nanoparticles. Electrospinning of the formed colloid results in producing the CoS nanoparticles inside the polymeric nanofibers. The obtained nanofibers have good catalytic activity toward dehydrogenation of ammonia borane. Moreover, the hybrid nanofibers are strongly recommended to be utilized as photocatalyst as the nanofibers could successfully photooxidize methlene blue dye in a very short time. Also, the stable azo dyes (e.g. methyl red) can be eliminated by exploiting the introduced nanofibers. The use of this kind of supported catalyst might avoid the need of secondary operations like liquid–solid separation.

Acknowledgment

This work was financially supported by the National Plan for Science & Technology (NPST), King Saud University Project no. 11-NAN1460-02. We thank Mr. T.S. Bae and J.C. Lim, KBSI, Jeonju branch, and Mr. Jong-Gyun Kang, Centre for University Research Facility, for taking high-quality FESEM and TEM images, respectively.

References

[1] H.H. Li, Z.R. Chen, J.Q. Li, C.C. Huang, Y.F. Zhang, G.X. Jia, Role of spacers and substituents in the self-assembly process: syntheses and characterization of three novel silver(I)/iodine polymers, Crystal Growth and Design 6 (2006) 1813–1820.
[2] J.F. Zhu, Y.J. Zhu, M.G. Ma, L.X. Yang, L. Gao, Simultaneous and rapid microwave synthesis of polyacrylamide – metal sulfide (Ag_2S, Cu_2S, HgS) nanocomposites, Journal of Physical Chemistry C 111 (2007) 3920–3926.
[3] G.C. Carotenuto, Y.S. Her, E. Matijevic, Preparation and characterization of nanocomposite thin films for optical devices, Industrial and Engineering Chemistry Research 35 (1996) 2929–2932.
[4] M.L. Cantú, P.G. Romero, Electrochemical and chemical synthesis of the hybrid organic–inorganic electroactive material formed by phosphomolybdate and polyaniline. Application as cation insertion electrode, Chemistry of Materials 10 (1998) 698–704.
[5] R. Krishnamoorti, R.A. Vaia, E.P. Giannelis, Structure and dynamics of polymer-layered silicate nanocomposites, Chemistry of Materials 8 (1996) 1728–1734.
[6] W. Caseri, Nanocomposites of polymers and metals or semiconductors: historical background and optical properties, Macromolecular Rapid Communications 21 (2000) 705–722.
[7] Y. Zhou, L.Y. Hao, Y. Hu, R.Y. Zhu, Z.K. Chen, Facile method to prepare metal sulfide(Ag_2S, CuS, PbS) nanoparticles grown on surface of polyacrylonitrile nanofibre and their optical properties, Chemistry Letters 28 (2000) 1308–1312.
[8] A. Gole, C.J. Murphy, Polyelectrolyte-coated gold nanorods: synthesis, characterization and immobilization, Chemistry of Materials 17 (2005) 1325–1330.
[9] G.B. Smith, A. Ignatiev, G. Za jac, Solar selective black cobalt: preparation, structure, and thermal stability, Journal of Applied Physics 51 (1980) 4186–4196.
[10] T.M. Whitney, J.S. Jiang, P. Searson, C. Chien, Fabrication and magnetic properties of arrays of metallic nanowires, Science 261 (1993) 1316–1319.
[11] G.H. Yue, P.X. Yan, X.Y. Fan, M.X. Wang, D.M. Qu, Z.G. Wu, C. Li, D. Yan, Structure and properties of cobalt disulfide nanowire arrays fabricated by electrodeposition, Electrochemical and Solid-State Letters 10 (2007) 29–31.
[12] Y.G. Feng, T. He, N. Alonso-Vante, In situ free-surfactant synthesis and ORR electro chemistry of carbon supported Co_3S_4 and $CoSe_2$ nanoparticles, Chemistry of Materials 20 (2008) 26–28.
[13] B.L. Davis, D.A. Dixon, E.B. Garner, J.C. Gordon, M.H. Matus, B.L. Scott, Efficient regeneration of partially spent ammonia borane fuel, Angewandte Chemie International 48 (2009) 6812–6816.
[14] D.H. Reneker, I. Chun, Nanometre diameter fibres of polymer produced by electrospinning, Nanotechnology 7 (1996) 216–223.
[15] W. He, Z. Ma, T. Yong, W.E. Teo, S. Ramakrishna, Fabrication of collagen-coated biodegradable polymer nanofiber mesh and its potential for endothelial cells growth, Biomaterials 26 (2005) 7606–7615.
[16] W.K. Son, J.H. Youk, W.H. Park, Antimicrobial cellulose acetate nanofibers containing silver nanoparticles, Carbohydrate Polymers 65 (2006) 430–434.

[17] X. Wang, C. Drew, S.H. Lee, K.J. Senecal, J. Kumar, L.A. Samuelson, Electrospun nanofibrous membranes for highly sensitive optical sensors, Nano letters 2 (2002) 1273–1275.
[18] A. Yousef, N.A.M. Barakat, T. Amna, S.S. Al-Deyab, M.S. Hassan, A. Abdel-hay, H.Y. Kim, Inactivation of pathogenic *Klebsiella pneumoniae* by CuO/TiO_2 nanofibers: a multifunctional nanomaterial via one-step electrospinning, Ceramics International 38 (2012) 4525–4532.
[19] A.R. Unnithan, N.A.M. Barakat, R. Nirmala, S.S. Al-Deyab, H.Y. Kim, Novel electrospun nanofiber mats as effective catalysts for water photosplitting, Ceramics International 38 (2012) 5175–5180.
[20] S. Xiao, M. Shen, R. Guo, S. Wang, X. Shi, Immobilization of zerovalent iron nanoparticles into electrospun polymer nanofibers: synthesis, characterization, and potential environmental applications, Journal of Physical Chemistry C 113 (2009) 18062–18068.
[21] S.A. Theron, E. Zussmana, A.L. Yarin, Experimental investigation of the governing parameters in the electrospinning of polymer solutions, Polymer 45 (2004) 2017–2030.
[22] M.C. Denney, V. Pons, T.J. Hebden, D.M. Heinekey, K.I. Goldberg, Efficient catalysis of ammonia borane dehydrogenation, Journal of the American Chemical Society 128 (2006) 12048–12049.
[23] O. Metin, V. Mazumder, S. Zkar, S. Sun, Monodisperse nickel nanoparticles and their catalysis in hydrolytic dehydrogenation of ammonia borane, Journal of the American Chemical Society 132 (2010) 1468–1469.
[24] M.E. Bluhm, M.G. Bradley, R. Butterick, U. Kusari, L.G. Sneddon, Amineborane-based chemical hydrogen storage: enhanced ammonia borane dehydrogenation in ionic liquids, Journal of the American Chemical Society 128 (2006) 7748–7749.
[25] A. Houas, H. Lachheb, M. Ksibi, Photocatalytic degradation pathway of methylene blue in water, Applied Catalysis B: Environmental 31 (2001) 145–157.